

# Estimating the performance of the GAPS detector with muon ground testing data from Antarctica

## A. Stoessl<sup>a,\*</sup> on behalf of the GAPS collaboration

<sup>a</sup>*Department of Physics and Astronomy,  
University of Hawaii at Manoa,  
2505 Correa Rd, Honolulu, HI 96822*

The General Antiparticle Spectrometer (GAPS) is a balloon-borne indirect dark matter experiment that was commissioned in Antarctica for the December 24/January 25 launch season. Its primary science goal is the search for light antinuclei in cosmic rays at kinetic energies below 0.25 GeV/ $n$ . This energy region is of particular interest for dark matter searches and remains largely unexplored. GAPS promises to yield unprecedented sensitivity for low-energy antideuterons, will measure the low-energy antiproton spectrum with high precision, and will open new discovery space for antihelium. To reach the required sensitivity, the GAPS detector incorporates a new approach for antimatter detection, utilizing a tracker with custom-designed, lithium-drifted Silicon detectors that both capture an incoming antinucleus into an exotic atom and measure the de-excitation X-ray and nuclear annihilation product, together with a fast time-of-flight system, allowing for a high-precision  $\beta$  measurement and trigger. During the past Antarctic season, GAPS performed a pre-flight, instrument testing campaign on the ground. Unfortunately, GAPS was not able to launch in the past season due to the weather. This talk will highlight key results from the Antarctic ground testing campaign and present an outlook for the December 2025/January 2026 Antarctic launch season in which GAPS is scheduled to launch.

39th International Cosmic Ray Conference (ICRC2025)  
15–24 July 2025  
Geneva, Switzerland



**ICRC 2025**

The Astroparticle Physics Conference  
Geneva July 15-24, 2025

---

\*Speaker

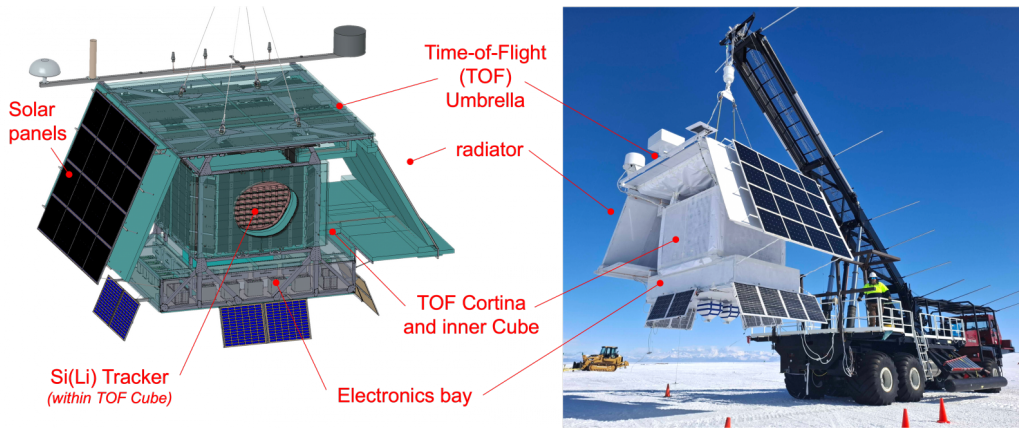


**Figure 1:** An overview of the GAPS instrument, with individual components indicated. The photograph shows GAPS as it is hung from the launch vehicle at the LDB site in McMurdo, Antarctica.

## 1. Introduction

The General Antiparticle Spectrometer (GAPS) is an indirect dark matter experiment optimized to detect low-energy ( $< 0.25 \text{ GeV}/n$ ) cosmic antiprotons [3], antideuterons [4], and antihelium [5] during a series of three Antarctic long-duration balloon (LDB) flights. Due to their ultra-low backgrounds, cosmic antinuclei heavier than antiprotons are excellent probes for dark matter models that predict dark matter annihilation or decay in the Galactic halo, including many models that evade detection in collider, direct, or other indirect searches [1]. An overview of the GAPS science goals can be found in further proceedings for this conference [2].

During the December 2024/January 2025 Antarctic launch season, GAPS was assembled, commissioned, and declared flight-ready; however, GAPS was ultimately unable to launch due to unfavorable weather conditions. Nevertheless, an extensive ground testing dataset has been collected, which, given the well-understood incident cosmic-ray muon flux, allows for instrument characterization based on the analysis of the recorded tracks. In addition, the long continuous runtime of the instrument allowed for extensive monitoring of system parameters and instrument health. These proceedings will discuss the results of the 2024/25 Antarctic ground testing campaign. GAPS remains assembled in Antarctica in anticipation of its first flight in the December 2025/January 2026 season.

## 2. The GAPS experiment

The instrument design of GAPS is motivated by the anticipated antiparticle event signature. An incoming primary antiparticle can annihilate within the detector, leaving a star-like pattern of secondaries along with the signature of its primary track. In addition to the hadronic annihilation products, for a capture at rest, an X-ray cascade from the formation of an exotic atom is expected [6].

As shown in Fig.1, the instrument has two different detector sub-systems, the innermost being a silicon tracker consisting of 10 cm diameter, 2.5 mm thick lithium-drift Silicon (Si(Li)) detectors [7–10]. The area of a single detector is segmented into eight equal-area strips. A custom ASIC

readout [11] has been developed to provide (i.) high-resolution X-ray spectroscopy ( $<5$  keV FWHM with 40 pF capacitance and  $<10$  nA leakage current for a single strip) over the range  $\approx 20$ – $100$  keV, (ii.) coarse-resolution spectroscopy ( $\approx 10\%$  FWHM) and tracking over the range  $1$ – $100$  MeV, and (iii.) coincidences of  $<1$   $\mu$ s between TOF and tracker. These detectors are grouped into modules, which, in addition to the front-end electronics, provide both electrical shielding and protection from ambient humidity. The modules are arranged into ten tracking planes, seven of which are populated with active Si(Li) detectors, and the other three planes provide target material. A novel oscillating heat pipe system [12, 13], along with a  $9$  m<sup>2</sup> radiator in conjunction with a rotator to keep it pointed away from the Sun, is used to cool the Si(Li) detectors to the requisite operational temperature ( $\approx -40$  °C).

The entire tracker is enclosed by a time-of-flight (TOF) system [14]. The TOF system consists of 160 plastic scintillator paddles, read out on both ends with Silicon PMTs, each with a high-gain channel for charge and timing measurement and a low-gain channel for the trigger system. A typical plastic scintillator paddle is 6.35 mm thick and 16 cm wide, with a few paddles of slightly different dimensions to achieve the best possible hermeticity by accommodating the actual gondola frame geometry. The TOF consists of an inner “cube” and outer “cortina” and “umbrella”. The cube encloses all six sides of the tracker system. The umbrella is a planar layer that is centered over the cube at a minimum distance of 90 cm, and the cortina surrounds the sides of the cube at a minimum distance of 30 cm. The distance between the umbrella and the cube is optimized to measure the velocity of the incident primary. The narrower spacing of the cortina allows for a compact design that accommodates the weight constraints of a balloon payload, while still providing sufficient velocity measurement of secondary particles. The TOF system provides a flexible trigger configuration. Trigger conditions are based on paddle locations, multiplicity, and the value of the crossed threshold of the scintillator signal. The specific trigger conditions set for the campaign are designed to trigger on incoming muon tracks (requiring at least one hit on both the inner and outer TOF) or the topology expected in flight for complex antinuclei interactions (at least eight hits total in the inner and outer TOF, at least three hits in each of the inner and outer TOF, and at least two hits satisfying a higher energy threshold). A dedicated TOF system computer and a custom-designed main trigger board orchestrate triggering and coordinate data taking for the different paddles. A publication detailing the GAPS instrument and readout system is in preparation.

### 3. GAPS instrument commissioning

GAPS was commissioned in Antarctica in late 2024, following an extensive period of technological development and validation. This included full thermal-vacuum testing at National Technical Systems (NTS) in Los Angeles, CA; mechanical upgrades and system-level testing at Columbia University’s Nevis Laboratories; and integration with NASA balloon components, followed by a final mission-readiness review at NASA’s Columbia Scientific Balloon Facility in Palestine, TX.

The GAPS team deployed to Antarctica’s McMurdo Station from November 2024 through January 2025. During flight preparation and integration, the GAPS experiment continuously recorded data to monitor its operation and performance. This allowed for testing of the individual components as soon as they were installed, as well as continuous monitoring of instrument health and operation parameters. Data recorded by the new components were integrated into the continuous instrument

data stream and stored in a database system for further offline processing. Improvements in software and operations, based on the experience of previous integration and calibration campaigns, were tested and validated. As soon as the Si(Li) tracker integration had been finished and the cooling system came online, the tracker was cooled down to operating temperature of  $-37^{\circ}\text{C}$  with the use of a dedicated ground cooling system using chillers with R23 coolant [13], allowing a testing campaign with an operational tracker for eight days. During this time, the inner TOF system was completed. During this combined system operation period, close to 100 million events were collected.

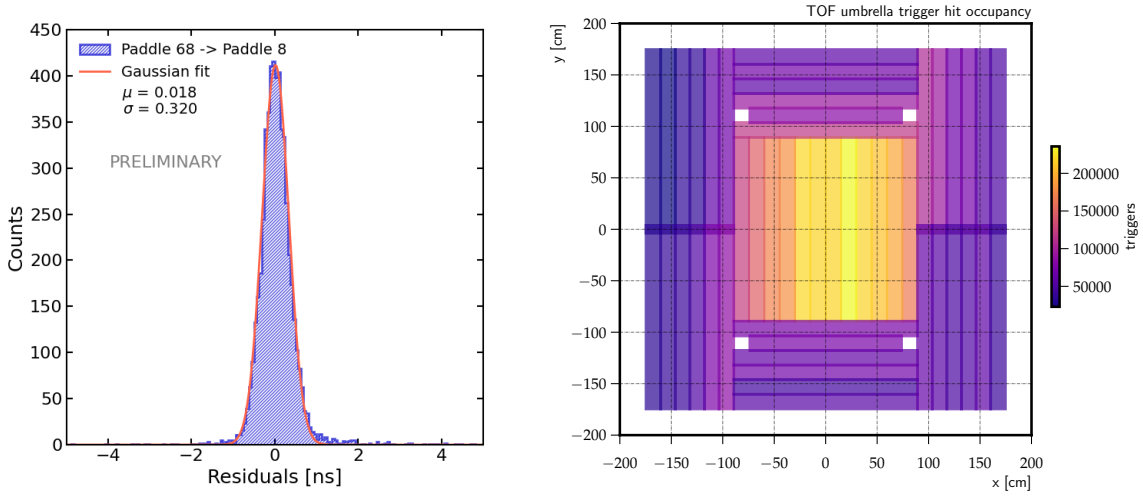
The particle flux on the ground is different than the actual signal for which the GAPS instrument has been designed. While muons on the ground mainly provide clean single tracks with a lower energy deposition than slow particles, the GAPS design was optimized for a star-like pattern emerging from the expected antimatter annihilation. For the ground cooling campaign, together with the high-multiplicity trigger, an additional trigger has been set, which is the requirement of only two hits, one on the inner and one on the outer TOF as mentioned in Sec. 2. Prescale factors for these two triggers allow for tuning the combined rate to 450-500Hz, which is approximately the rate expected in flight as well. The high-multiplicity trigger stream, albeit recorded at a low rate of a few Hz, helps study event signatures as they would appear as background events in an antinuclei search and for testing the functionality of the annihilation star reconstruction [15]. An online algorithm that prioritizes telemetry to ground of antinuclei candidate events, based on more detailed criteria for TOF hits and tracker energy depositions, was also validated. This online event pre-selection may become crucial in cases where the disks on the gondola cannot be recovered after the flight, or the bandwidth for telemetry during the flight is too low to accommodate the expected data rate.

#### 4. Instrument performance

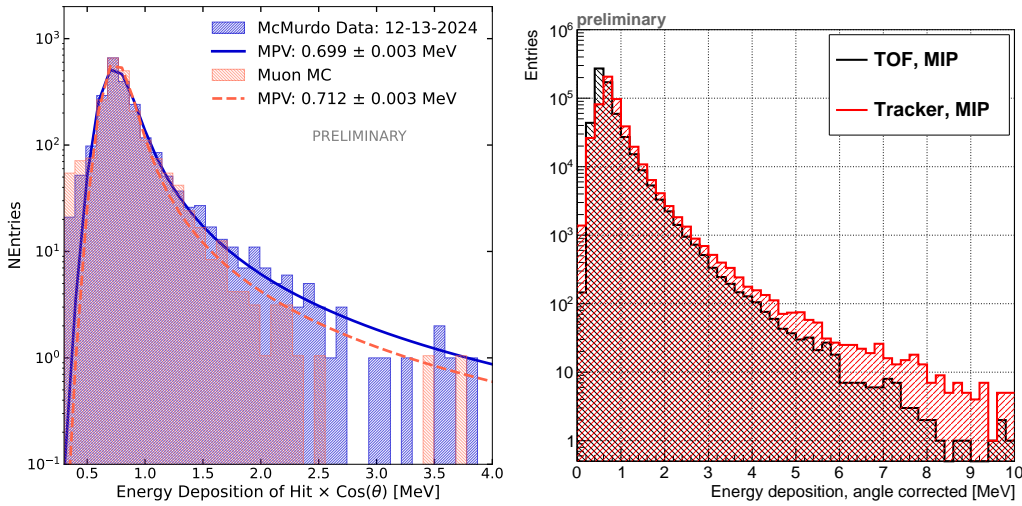
The recorded muon signal provides a sample of clean, single-track events. Such a sample can be extracted by applying simple filter criteria to the data, e.g., requiring a minimum number of hits in the individual tracker layers and a certain ordering of the TOF hits in time. These quantities allow the construction of track samples that can be used for detector performance studies.

Fig. 2 shows the occupancy of the TOF umbrella for all triggered events before any additional selection. Differences in paddle occupancy stem from the different areas of the paddles in the different sections of the umbrella. The effect of the trigger efficiency due to the geometry is clearly visible and has been compared with simulations. The simulation exhibits the same pattern for occupancy as recorded in the data, thus verifying the effect of the geometry trigger acceptance. For every paddle in the TOF, the full waveform is digitized and recorded, but to save bandwidth during flight, an online pulse extraction algorithm is run. The ground testing campaign allows comparison of waveforms with the result of this pulse extraction algorithm in situ.

Selecting down-going tracks allows studying the alignment of tracker detectors. For that purpose, the distribution of the residuals of the track intersection points with the respective layers and the position of the measured hits can be investigated, as shown in Fig. 4. The tight distribution, whose variance is on the order of the width of a tracker strip, shows no indication of displacement of the individual tracker layers. A possible rotation and the alignment between TOF and tracker are currently under active investigation. An example of a straight down-going muon track is shown in Fig. 4. The energy deposition along the path of the track provides a crucial parameter for iden-



**Figure 2:** *Left:* Time-of-flight for two paddles on top of each other at a distance of about 1m. The expected muon flight time has been subtracted. *Right:* Trigger occupancy of the TOF umbrella.



**Figure 3:** *Left:* Comparison of data and simulation energy depositions along single-track events correct for zenith angle in one tracker detector. *Right:* Energy depositions in all TOF and tracker detectors along single-track events correct for zenith angle.

tifying the incident primary, as  $dE/dx$  is given by the Bethe-Bloch formula. The zenith-weighted energy deposition for TOF and tracker is shown in Fig. 2. To identify a particle by its mass and charge through the  $dE/dx$  method, a precise measurement of particle velocity  $\beta$  is essential, since  $dE/dx \propto 1/\beta^2$ . The GAPS TOF system was designed to achieve a timing resolution of about 500 ps. The design goal was verified in lab measurements and with the GAPS prototype. Verification of these previous measurements has been performed and provides consistent results, as demonstrated in Fig. 2. The narrow timing distribution demonstrates that GAPS satisfies its TOF design goals.

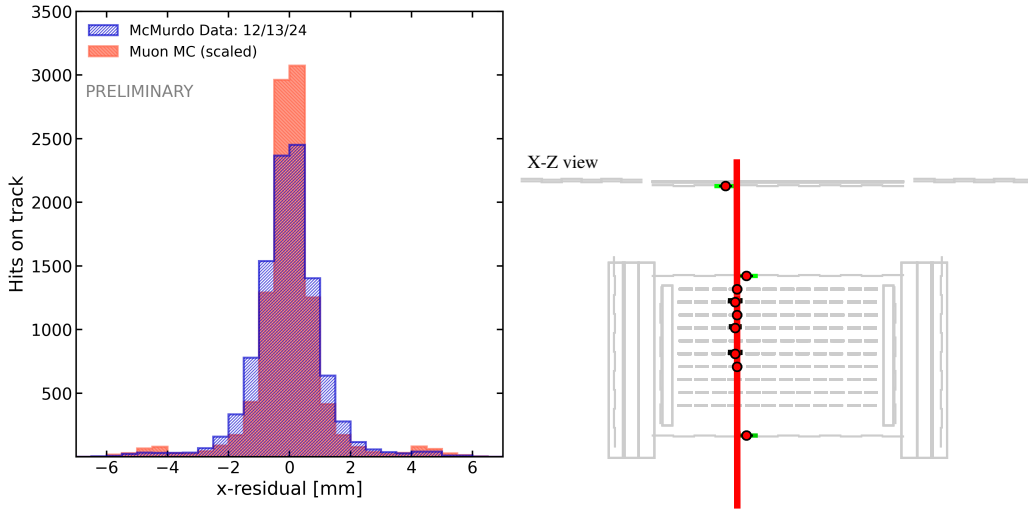


**Figure 4:** *Left:* Position residual of tracker strip position and reconstructed track for straight downgoing events. *Right:* A straight downgoing muon. Recorded energy deposition indicated by the color scale

## 5. Conclusion

During its commissioning for the anticipated flight during the December 2025/January 2026 Antarctic launch season, the GAPS experiment recorded an extensive ground dataset, despite challenging weather conditions and a tight schedule. While different than the anticipated antiparticle signal, the atmospheric muon flux provides a high-statistics sample to validate key detector performance requirements, online algorithms, tracker alignment, as well as probing crucial identification parameters for the incoming primary particle. The recorded data are actively studied by the GAPS collaboration and provide valuable input for the preparation of the upcoming launch in the 2025/2026 Antarctic season.

## Acknowledgements

This work is supported in the U.S. by NASA Astrophysics Research and Analysis GAPS grants (NNX17AB44G, NNX17AB46G, NNX17AB47G, 80NSSC21K1877) PI, C. Hailey, in Japan by JAXA/ISAS Small Science Program FY2017, and in Italy by Istituto Nazionale di Fisica Nucleare (INFN) and by the Italian Space Agency through the ASI INFN agreement n. 2018-28-HH.0: "Partecipazione italiana al GAPS - General AntiParticle Spectrometer". H. Fuke is supported by JSPS KAKENHI grants (JP17H01136, JP19H05198, JP22KK0042, and JP22H00147). K. Perez, G. Bridges, K. Pappas, and S. Vickers are also supported by Heising-Simons Foundation awards 2023-4617 and 2025-6055. R. A. Ong receives support from the UCLA Division of Physical Sciences. This work is partially supported by the U.S. Department of Energy, Office of Science, under contract number DE-AC05-00OR22725. Sydney Feldman was supported through the National Science Foundation Graduate Research Fellowship under grant 2034835. The contributions of C. Gerrity were supported by NASA under award No. 80NSSC19K1425 of the Future Investigators in NASA Earth and Space Science and Technology (FINESST) program. K. Yee is supported

through the National Science Foundation Graduate Research Fellowship under grant 2141064. K. Aoyama receives support from JSPS KAKENHI grant JP24K22891. K. Mizukoshi receives support from JSPS KAKENHI grants (JP22K20375 and JP24K17079). S. Okazaki receives support from JSPS KAKENHI grants (JP18K13928 and JP22KK0042). Y. Shimizu receives support from JSPS KAKENHI grants (JP20K04002, JP22KK0042, JP23K03436). M. Xiao, Z. Wu, and J. Yang receive support from the Yangyang Development Fund. The technical support and advanced computing resources from the University of Hawaii Information Technology Services – Research Cyberinfrastructure, funded in part by the National Science Foundation CC\* awards #2201428 and #2232862, are gratefully acknowledged. This research was done using services provided by the OSG Consortium [16–19], which is supported by the National Science Foundation awards #2030508 and #2323298. We express our sincere thanks to the NASA Columbia Scientific Balloon Facility and the National Science Foundation United States Antarctic Program for their professional support throughout the balloon flight preparation.

## References

- [1] P.v. Doetinchem et al., *Journal of Cosmology and Astroparticle Physics* **2020** (2020) 035.
- [2] K. Yee et al., Antinuclei Signatures of Dark Matter and the GAPS Experiment, *these proceedings*.
- [3] F. Rogers et al., *Astroparticle Physics* **145** (2023) 102791
- [4] T. Aramaki et al., *Astroparticle Physics* **74** (2016) 6-13
- [5] N. Saffold et al., *Astroparticle Physics* **130** (2021) 102580.
- [6] C.J. Hailey et al., *New Journal of Physics* **11** (2009) 105022.
- [7] M. Xiao et al., *IEEE Transactions on Nuclear Science* **8** (2023) 2125.
- [8] M. Kozai et al., *Nucl. Instrum. Meth. A* **947** (2019) 2695 [1906.05577].
- [9] F. Rogers et al., *Journal of Instrumentation* **14** (2019) P10009.
- [10] K. Perez et al., *Nucl. Instrum. Meth. A* **905** (2018) 12 [1807.07912].
- [11] M. Manghisoni et al., *IEEE Transactions on Nuclear Science* **71** (2024).
- [12] H. Fuke et al., *Nucl. Instr. and Methods A* **1049** (2023) 168102
- [13] K. Aoyama et al., GAPS Detector Cooling System: Results from Antarctic Ground Tests, *these proceedings*.
- [14] T. Aramaki et al., *GAPS contributions to the 38th International Cosmic Ray Conference* (2023)
- [15] R. Munini et al., *Astroparticle Physics* **133** (2021) 10264

- [16] R. Pordes et al., *J. Phys. Conf. Ser.* **78** (2007) 012057
- [17] I. Sfiligoi et al., *2009 WRI World Congress on Computer Science and Information Engineering* **2** (2009) 428–432
- [18] OSG, *OSPool* (2006)
- [19] OSG, *Open Science Data Federation* (2015)

K. Aoyama<sup>1</sup>, T. Aramaki<sup>2</sup>, P. Beggs<sup>3</sup>, M. Boezio<sup>4,5</sup>, S. E. Boggs<sup>6</sup>, G. Bridges<sup>7</sup>, V. Bonvicini<sup>4</sup>, D. Campana<sup>8</sup>, E. Everson<sup>3</sup>, L. Fabris<sup>9</sup>, S. Feldman<sup>3</sup>, H. Fuke<sup>1</sup>, F. Gahbauer<sup>7</sup>, C. Gerrity<sup>10</sup>, L. Ghisloti<sup>11,12</sup>, C. J. Hailey<sup>7</sup>, T. Hayashi<sup>3</sup>, A. Kawachi<sup>13</sup>, K. Konoma<sup>13</sup>, M. Kozai<sup>2,5</sup>, P. Lazzaroni<sup>11</sup>, A. Lowell<sup>14</sup>, M. Manghisoni<sup>11,12</sup>, M. Martucci<sup>15</sup>, K. Mizukoshi<sup>17</sup>, E. Mocchiutti<sup>4</sup>, B. Mochizuki<sup>14</sup>, K. Munakata<sup>18</sup>, R. Munini<sup>4,5</sup>, S. Okazaki<sup>1</sup>, R. A. Ong<sup>3</sup>, G. Osteria<sup>8</sup>, F. Palma<sup>15</sup>, K. Pappas<sup>7</sup>, K. Perez<sup>7</sup>, F. Perfetto<sup>8,19</sup>, L. Ratti<sup>11,12</sup>, V. Re<sup>11,12</sup>, E. Riceputi<sup>11,12</sup>, F. Rogers<sup>14</sup>, S. Sakamoto<sup>20</sup>, P. Sawant<sup>15,16</sup>, V. Scotti<sup>8,19</sup>, Y. Shimizu<sup>20</sup>, R. Sparvoli<sup>15,16</sup>, A. Stoessl<sup>10</sup>, A. Suraj<sup>2</sup>, A. Tiberio<sup>21,22</sup>, G. Tytus<sup>10</sup>, E. Vannuccini<sup>21</sup>, S. Vickers<sup>7</sup>, P. von Doetinchem<sup>10</sup>, L. Volpicelli<sup>15,16</sup>, Z. Wu<sup>23</sup>, M. Xiao<sup>23</sup>, J. Yang<sup>23</sup>, K. Yee<sup>7,24</sup>, T. Yoshida<sup>1</sup>, G. Zampa<sup>4</sup>, J. Zeng<sup>2</sup>, and J. Zweerink<sup>3</sup>

<sup>1</sup>Institute of Space and Astronautical Science, Japan Aerospace Exploration Agency (ISAS/JAXA), Sagami-hara, Kanagawa 252-5210, Japan. <sup>2</sup>Northeastern University, 360 Huntington Avenue, Boston, MA 02115, USA. <sup>3</sup>University of California, Los Angeles, Los Angeles, CA 90095, USA. <sup>4</sup>INFN, Sezione di Trieste, I-34149 Trieste, Italy. <sup>5</sup>IFPU, I-34014 Trieste, Italy. <sup>6</sup>University of California, San Diego, La Jolla, CA 90037, USA. <sup>7</sup>Columbia University, New York, NY 10027, USA. <sup>8</sup>INFN, Sezione di Napoli, I-80126 Naples, Italy. <sup>9</sup>Oak Ridge National Laboratory, Oak Ridge, TN 37831, USA. <sup>10</sup>University of Hawaii at Manoa, Honolulu, HI 96822 USA. <sup>11</sup>INFN, Sezione di Pavia, I-27100 Pavia, Italy. <sup>12</sup>Università di Bergamo, I-24044 Dalmine (BG), Italy. <sup>13</sup>Tokai University, Hiratsuka, Kanagawa 259-1292, Japan. <sup>14</sup>Space Sciences Laboratory, University of California, Berkeley, 7 Gauss Way, Berkeley, CA 94720, USA. <sup>15</sup>Università di Trieste, I-34127 Trieste, Italy. <sup>16</sup>INFN, Sezione di Roma "Tor Vergata", I-00133 Rome, Italy. <sup>17</sup>Università di Roma "Tor Vergata", I-00133 Rome, Italy. <sup>18</sup>Tohoku University, Aoba-6-3 Aramaki, Aoba Ward, Sendai, Miyagi 980-8578, Japan. <sup>19</sup>Shinshu University, Matsumoto, Nagano 390-8621, Japan. <sup>20</sup>Università di Napoli "Federico II", I-80138 Naples, Italy. <sup>21</sup>Kanagawa University, Yokohama, Kanagawa 221-8686, Japan. <sup>22</sup>INFN, Sezione di Firenze, I-50019 Sesto Fiorentino, Florence, Italy. <sup>23</sup>Università degli Studi Firenze, 50121 Firenze FI, Italy. <sup>24</sup>School of Physics and Astronomy, Shanghai Jiao Tong University, Key Laboratory for Particle Astrophysics and Cosmology (MoE), Shanghai Key Laboratory for Particle Physics and Cosmology, 800 Dongchuan RD. Minhang District, Shanghai 200240, China. <sup>25</sup>Massachusetts Institute of Technology, Cambridge, MA 02139, USA. <sup>26</sup>Research Organization of Information and Systems, 4 Chome-3-13 Toranomon, Minato City, Tokyo 105-0001, Japan.